Applied Catalysis B: Environmental 91 (2009) 428–433

Contents lists available at ScienceDirect

Applied Catalysis B: Environmental

journal homepage: www.elsevier.com/locate/apcatb

Composition optimization of PtRuM/C (M = Fe and Mo) catalysts for methanol electro-oxidation via combinatorial method

Ki Rak Lee, Min Ku Jeon [1], Seong Ihl Woo *

Department of Chemical and Biomolecular Engineering (BK21 Graduate Program) & Center for Ultramicrochemical Process Systems (CUPS), Korea Advanced Institute of Science and Technology, 373-1 Gusong-dong, Yuseong-gu, Daejeon 305-701, Republic of Korea

ARTICLE INFO

Article history:
Received 11 March 2009
Received in revised form 15 June 2009
Accepted 15 June 2009
Available online 23 June 2009

Keywords:
Methanol electro-oxidation
Direct-methanol fuel cell
Combinatorial chemistry
High-throughput screening

ABSTRACT

Ternary PtRuFe and PtRuMo alloy systems were investigated for methanol electro-oxidation reaction (MOR). Rapid optimization of the ternary alloy compositions was achieved via combinatorial synthesis and high-throughput screening method. A combinatorial library was composed of 121 different compositions of the ternary PtRuFe and PtRuMo alloys. High MOR activities were observed in $Pt_5Ru_3Fe_2$, $Pt_4Ru_3Fe_3$, $Pt_5Ru_4Mo_1$ and $Pt_4Ru_4Mo_2$ compositions (mass ratio) via quantitative analysis of each catalyst spots. Performances of these compositions were verified in their powder version catalysts: (1) on-set potential for CO electro-oxidation decreased by 0.05 V in the PtRuFe alloys and 0.15 V in the PtRuMo and (2) high MOR activities were observed in the $Pt_5Ru_4Fe_1$/C (98% higher mass activity than that of commercial PtRu/C) and the $Pt_4Ru_3Mo_3$/C (260% higher specific activity than that of commercial PtRu/C).

1. Introduction

Direct-methanol fuel cell (DMFC) is one of the most practical fuel cells, because methanol can be stored and transported more safely than hydrogen. Therefore, intensive research on the DMFC has been carried out [1–5]. However, the use of methanol suffers from obstacles such as poor electro-catalytic activity at the anode electrode and cross-over of methanol from the anode to the cathode electrode [6,7]. In order to solve these problems, many studies have been focused on the development of highly active catalysts for methanol electro-oxidation reaction (MOR) [2]. Pt–Ru alloy catalyst is still considered as one of the best catalysts for the MOR until now.

In the PtRu alloy catalyst, Ru plays an important role to improve CO tolerance property of pure Pt. The pure Pt catalyst shows high activity for the MOR, but a rapid drop of activity is followed because of poisoning by adsorbed CO (CO_{ads}) which is an intermediate of the MOR. Under the “bi-functional mechanism” as shown below, Ru dissociates water to produce Ru–OH to react with CO_{ads} [8,9]:

$$Pt + CH_3OH \rightarrow Pt{-}CO + 4H^+ + 4e^- \quad (1)$$

$$Ru + H_2O \rightarrow Ru{-}OH + H^+ + e^- \quad (2)$$

$$Pt{-}CO + Ru{-}OH \rightarrow Pt + Ru + CO_2 + H^+ + e^- \quad (3)$$

Although the PtRu catalysts exhibit much higher MOR activity than that of pure Pt, further investigation on the MOR catalyst is desirable due to relatively low catalytic activity of the PtRu catalysts and economic burden of expensive Pt and Ru. For further improvement, various solutions such as core shell structure [10,11], ternary and quaternary catalysts [12–16], nanowire [17], and ultra-fine particle [18,19], were introduced. In a recent review [20], Demirci carried out theoretical study for the MOR and carefully suggested the incorporation of a third metal as the best way to improve the MOR activity. So far, various Pt–Ru based ternary catalysts have been introduced as promising MOR catalysts: such as PtRuCu [21], PtRuNi [13,22], PtRuIr [23], PtRuW [24,25], PtRuCo [24,26] PtRuFe [12,27], and PtRuMo [28,29]. In this study, we selected Fe and Mo as a third component. Previously, we reported that the PtRuFe catalyst is a promising catalyst for the MOR [12,27]. In the case of the PtRuMo system, we observed reduced MOR activity in our previous study [28], while other reports suggested PtRuMo as a promising MOR catalyst [29,30]. Watanabe et al. [31] reported the improved CO tolerance property in PtFe and PtMo binary catalysts. In addition, Mo was reported to

* Corresponding author. Tel.: +82 42 869 3918; fax: +82 42 869 8890.
E-mail address: siwoo@kaist.ac.kr (S.I. Woo).
[1] Present address: Department of Chemical and Biomolecular Eng., University of Notre Dame, Notre Dame, IN 46556, USA.

0926-3373/$ – see front matter.
doi:10.1016/j.apcatb.2009.06.011

reduce on-set potential for CO electro-oxidation in its PtMo binary alloy form [32,33]. In spite of their technical importance, neither of the PtRuFe and PtRuMo systems was investigated for their optimum composition for the MOR. However, optimization of a ternary system is a time- and cost-consuming procedure due to too many compositions to be explored. The best way in lessening the time and decreasing the cost is to employ combinatorial chemistry and high-throughput screening techniques.

Initially, the combinatorial chemistry and high-throughput screening techniques have been developed and are extensively being applied in the drug industry. These techniques have been first applied in the fuel cell research by Reddington et al. [34]. Since then, various combinatorial methods have been applied for rapid and efficient development of new MOR catalysts. Sputtering is a popular way to produce combinatorial library due to quick and accurate preparation of tens of samples [24]. Other rapid synthesis methods have been developed including physical vapor deposition [26,35], electro-deposition [36], and solution dispensing [16,34,37]. With the development of library synthesis methods, various high-throughput screening methods also have been evolved including optical screening [16,34,37], scanning electrochemical microscopy [38], multi-electrode half cell [39,40], and multi-electrode fuel cell [41]. However, single cell performance is sometimes not consistent with "optimized" combinatorial results because catalysts utilization is often sensitive to the synthesis method. To reduce this gap, Smotkin et al. [42] suggested a state-of-the-art combinatorial technique which evaluated every spots in as near to realistic fuel cell conditions as possible. However, number of library is rather limited in this method.

In this study, we introduced a new library preparation method, which is a similar with powder version catalysts synthesis by conventional $NaBH_4$ reduction [43]. Suggested method is expected to show accordance with real fuel cell test due to this similarity. Quantitative evaluation of each spot was performed by three electrode half cell method which was previously adopted by Jiang and Chu [44]. As noted above, Fe and Mo were chosen as a third member of the PtRu catalyst to prepared two systems of the ternary PtRuFe and PtRuMo alloys in one library. To verify the feasibility of the results obtained from the combinatorial library, optimized compositions were also synthesized and characterized in their powder form.

2. Experimental

2.1. Preparation of PtRuM/C (M = Mo and Fe) combinatorial library

121 (11 × 11) carbon spots were deposited by spraying carbon ink through a stainless-steel mask on a polytetrafluoroethylene (PTFE) treated carbon paper (Toray TGPH-090, 20 wt.% PTFE). The carbon ink was prepared by mixing carbon powder (Vulcan XC72R), de-ionized (DI) water, 5 wt.% Nafion ionomer solution, and isopropyl alcohol. Diameter of the catalyst spots was 4 mm. Then, the catalyst precursor solutions were deposited on the carbon spots. To make composition gradient, four precursor solutions of Pt, Ru, Fe, and Mo were prepared separately by using chloroplatinic acid hydrate, ruthenium (III) chloride, ammonium iron (II) sulfate hexahydrate, and ammonium molybdate tetrahydrate, respectively. Each solution was dripped on the carbon spots for various times to make 10 wt.% composition change for each spot. After drying at room temperature, the library was reduced by soaking in 0.2 M $NaBH_4$ solution for 2 h. The reduced library was washed with DI water to remove reduction residues. The picture of the final library is shown in Fig. 1 and the composition of each spot is shown in Table 1. Binary PtRu compositions are represented diagonally in Table 1. The other binary compositions of Pt–Fe, Pt–Mo, Ru–Fe, and Ru–Mo are shown along the four sides of Table 1. Total loading of the metals was adjusted to 34 wt.%. All metal ratios in this paper are shown in weight basis.

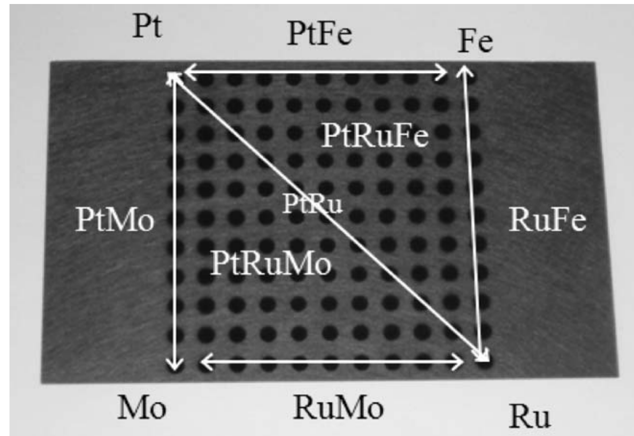

Fig. 1. A picture of the combinatorial library which includes 121 different compositions of ternary PtRuM (M = Fe or Mo) catalysts.

2.2. Measurement of MOR electrochemical activity with combinatorial library

Each catalyst spot on the combinatorial library worked as a working electrode. Platinum wire and Ag/AgCl electrode (BAS Co., Ltd., MF2052 RE-5B) were used as the counter and reference electrodes, respectively. To separate electrolyte and measure MOR activity of each catalyst spot, we used a PTFE mask which has 121 holes with 5 mm diameter and 10 mm depth. The counter and reference electrodes were put in each hole and the MOR activity measurement was performed. After measuring one spot, the counter and reference electrodes were moved to the next spot. The MOR activity measurement was performed by potential cycling between 0 and 0.8 V (vs. reference hydrogen electrode (RHE)) at a scan rate of 30 mV/s for 3 times. Nitrogen purged the solution containing 1 M of methanol and sulfuric acid. To prevent oxygen dissolution during the tests, the MOR activity measurement was

Table 1
Compositions of the combinatorial library are shown in Fig. 1 denoted by weight ratio of Pt:Ru:Fe:Mo.

10:0:0:0	9:0:1:0	8:0:2:0	7:0:3:0	6:0:4:0	5:0:5:0	4:0:6:0	3:0:7:0	2:0:8:0	1:0:9:0	0:0:10:0
9:0:0:1	9:1:0:0	8:1:1:0:	7:1:2:0:	6:1:3:0	5:1:4:0	4:1:5:0	3:1:6:0	2:1:7:0	1:1:8:0	0:1:9:0
8:0:0:2	8:1:0:1	8:2:0:0	7:2:1:0	6:2:2:0	5:2:3:0	4:2:4:0	3:2:5:0	2:2:6:0	1:2:7:0	0:2:8:0
7:0:0:3	7:1:0:2	7:2:0:1	7:3:0:0	6:3:1:0	5:3:2:0	4:3:3:0	3:3:4:0	2:3:5:0	1:3:6:0	0:3:7:0
6:0:0:4	6:1:0:3	6:2:0:2	6:3:0:1	6:4:0:0	5:4:1:0	4:4:2:0	3:4:3:0	2:4:4:0	1:4:5:0	0:4:6:0
5:0:0:5	5:1:0:4	5:2:0:3	5:3:0:2	5:4:0:1	5:5:0:0	4:5:1:0	3:5:2:0	2:5:3:0	1:5:4:0	0:5:5:0
4:0:0:6	4:1:0:5	4:2:0:4	4:3:0:3	4:4:0:2	4:5:0:1	4:6:0:0	3:6:1:0	2:6:2:0	1:6:3:0	0:6:4:0
3:0:0:7	3:1:0:6	3:2:0:5	3:3:0:4	3:4:0:3	3:5:0:2	3:6:0:1	3:7:0:0	2:7:1:0	1:7:2:0	0:7:3:0
2:0:0:8	2:1:0:7	2:2:0:6	2:3:0:5	2:4:0:4	2:5:0:3	2:6:0:2	2:7:0:1	2:8:0:0	1:8:1:0	0:8:2:0
1:0:0:9	1:1:0:8	1:2:0:7	1:3:0:6	1:4:0:5	1:5:0:4	1:6:0:3	1:7:0:2	1:8:0:1	1:9:0:0	0:9:1:0
0:0:0:10	0:1:0:9	0:2:0:8	0:3:0:7	0:4:0:6	0:5:0:5	0:6:0:4	0:7:0:3	0:8:0:2	0:9:0:1	0:10:0:0

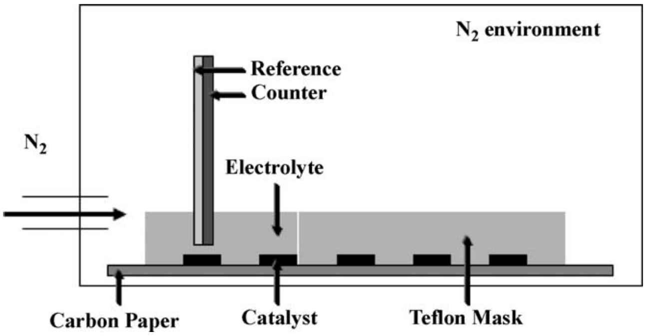

Fig. 2. Schematic diagram of the measurement set-up for electrochemical analysis of the combinatorial library.

performed under nitrogen flow. Schematic diagram of the experimental set-up is shown in Fig. 2. All potentials in this paper were converted to RHE scale.

2.3. Preparation of optimized MOR electrocatalysts

Pt:Ru:Mo (5:3:2 and 4:3:3) and Pt:Ru:Fe (5:4:1 and 4:4:2) compositions were prepared in their powder version. We used conventional $NaBH_4$ reduction method to prepare the powder version catalysts [43]. Carbon support (Vulcan XC72R) was dispersed in a mixture of DI water and isopropyl alcohol. Then appropriate amount of precursors were dissolved in the mixture. The same precursors used in the library preparation were used. The mixture was stirred for 1 h at 80 °C. Reduction was performed by adding 0.2 M $NaBH_4$ solution to the mixture, and then the mixture was further stirred for 3 h to complete the reduction reaction. The mixture was filtered and washed with DI water. The final catalyst powder was dried at 100 °C in an oven overnight. The synthesized catalysts were named as $Pt_5Ru_3Mo_2$/C, $Pt_4Ru_3Mo_3$/C, $Pt_5Ru_4Fe_1$/C, and $Pt_4Ru_4Fe_2$/C corresponding to their mass ratio. Loading of metals was 60 wt.%.

2.4. Electrochemical characterization of the powder version catalysts

Electrochemical studies were performed in a beaker-type three electrode cell. The working electrodes were prepared by the thin-film electrode method [45]. The catalysts were dispersed in DI water, followed by sonication. And then the catalyst dispersion was dripped on a glassy carbon electrode (3 mm diameter, BAS Co., Ltd., MF-2012). After drying at room temperature, 5 wt.% Nafion ionomer solution was dripped on the glassy carbon working electrode to stabilize the catalyst layer. The catalysts were tested for CO stripping and MOR activity. The CO stripping experiments were performed by measuring desorption performance of pre-adsorbed CO. CO was adsorbed on the catalyst by bubbling CO through the cell for 1 h while keeping the working electrode at 0.1 V. Excess CO was removed by N_2 purge through the cell for 50 min. The adsorbed CO was desorbed by potential increase up to 1.2 V and then the potential was cycled between 1.2 and 0 V at a scan rate of 15 mV/s. The MOR activity was measured after 30 potential cycling between 0 and 0.8 V at a scan rate of 15 mV/s in 1 M H_2SO_4 and 1 M methanol. Chronoampherommetry experiments were performed by keeping the working electrodes at 0.5 V for 1500 s. 1 M H_2SO_4 + 1 M methanol solution was used as the electrolyte. All experiments were conducted at 25 °C.

X-ray diffraction (XRD, D/MAX-IIIC diffractometer, Rigaku Co.) was performed using CuKα radiation for characterization of structural properties of the powder catalysts.

3. Results and discussions

Table 2 shows the MOR activity measurement results of the combinatorial library. In the PtRu binary system, the highest MOR activity (2.29×10^{-3} A/cm^2) was observed at Pt_8Ru_2. Equivalent atomic ratio of Pt to Ru for Pt_8Ru_2 is 2:1. It was reported that Pt_2Ru_1 in bulk composition which was lower Ru composition exhibits the highest activity at room temperature [26,46]. Our library result is in agreement with previous study. However, the highest activity was attained with PtRu black (the atomic ratio of Pt to Ru = 1) above 60 °C [46–48]. The non-Pt alloys of Ru–Mo and Ru–Fe region did not show any response to the MOR test, which means they are not active for the MOR and Pt is essential for the MOR. In the Pt–Fe binary compositions, we could observe higher MOR activity when Fe loading was between 10 and 30 wt.%. However, when Fe loading was higher than 40 wt.%, the MOR activity decreased drastically. The improved MOR activity of the PtFe catalyst was reported previously [49], and our results show that the maximum activity was obtained at 30 wt.% loading. In the Pt–Mo binary compositions, slightly higher MOR activity than the pure Pt catalyst was observed in Pt_8Mo_2 composition by weight. But the rest of the compositions exhibited the same or lower MOR activity than that of the pure Pt catalyst, which means that Mo is not a good candidate as a second metal to improve the MOR of pure Pt catalyst. In the ternary (PtRuMo and PtRuFe) composition regions, we could observe that most of them exhibited MOR activity higher than pure Pt catalyst. And MOR activity higher than (2.29×10^{-3} A/cm^2) of the best PtRu composition (Pt_8Ru_2) was observed in some compositions, such as $Pt_5Ru_3Mo_2$ (3.04×10^{-3} A/cm^2), $Pt_4Ru_3Mo_3$ (3.09×10^{-3} A/cm^2), $Pt_5Ru_4Fe_1$ (3.37×10^{-3} A/cm^2), and $Pt_4Ru_4Fe_2$ (3.10×10^{-3} A/cm^2). These unusually high activities were confirmed with their powder version catalysts.

Fig. 3 shows the XRD patterns of the powder version catalysts including commercial PtRu/C catalyst ("PtRu/C", E-tek, 60 wt.%, Pt:Ru = 1:1 atomic ratio) for comparison. Analysis of the structural

Table 2
Current density values of the combinatorial library at 0.5 V (unit is mA/cm^2).

0.37	1.75	0.76	1.80	0.29	0.26	0.13	0.25	0.06	0.095	0
0.17	0.18	0.89	1.05	2.27	1.71	0.58	0.81	0.73	0.5	0
0.45	1.82	2.29	2.31	2.51	1.42	0.92	1.30	0.98	0.37	0
0.22	1.30	2.48	2.24	1.58	2.22	1.15	1.70	1.13	0.51	0
0.37	0.50	1.71	1.63	1.64	3.37[a]	3.10[b]	1.95	1.30	0.67	0
0.13	1.15	1.81	3.04[c]	1.62	1.9	1.68	2.4	1.60	0.95	0
0.06	0.38	1.90	3.09[d]	1.24	1.2	2.04	1.69	1.60	1.15	0
0.08	0.41	1.62	2.30	1.99	1.44	1.46	1.77	1.80	0.90	0
0.12	0.53	1.36	1.53	1.87	1.04	1.00	0.93	1.30	0.72	0
0.02	1.18	0.95	1.80	1.90	1.60	0.84	0.84	1.20	0.98	0
0	0	0	0	0	0	0	0	0	0	0

[a] $Pt_5Ru_4Fe_1$.
[b] $Pt_4Ru_4Fe_2$.
[c] $Pt_5Ru_3Mo_2$.
[d] $Pt_4Ru_3Mo_3$.

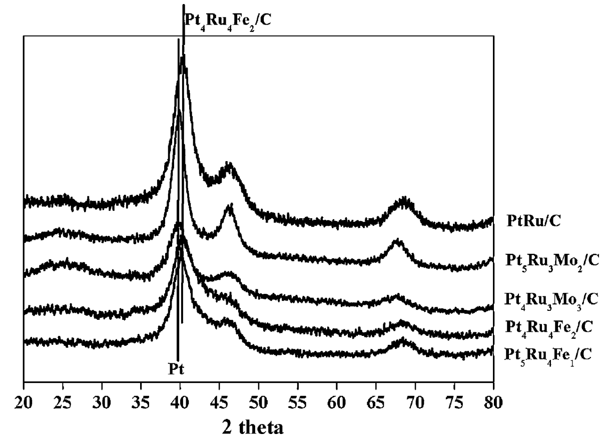

Fig. 3. XRD patterns of the powder catalysts: PtRu/C, $Pt_5Ru_3Mo_2/C$, $Pt_4Ru_3Mo_3/C$, $Pt_4Ru_4Fe_2/C$, and $Pt_5Ru_4Fe_1/C$.

Table 3
A summary of structural properties of the powder version catalysts.

Catalysts	(1 1 1) peak position (°)	*d* (Å)	Crystallite size (nm)
PtRu/C	40.24	2.245	3.1
$Pt_5Ru_4Fe_1/C$	40.08	2.253	3.0
$Pt_4Ru_4Fe_2/C$	40.36	2.238	2.9
$Pt_4Ru_3Mo_3/C$	39.80	2.268	3.3
$Pt_5Ru_3Mo_2/C$	39.90	2.263	3.4

properties was performed based on the (1 1 1) peak which was observed at 40.24° in the PtRu/C catalyst. In the PtRuFe catalysts, the (1 1 1) peak was observed at 2θ values of 40.08° for $Pt_5Ru_4Fe_1$ and 40.36° for $Pt_4Ru_4Fe_2$ catalysts higher than Pt, indicating the alloying of small Fe atoms. On the other hand, the (1 1 1) peak moved to the 2θ values of 39.80° for $Pt_4Ru_3Mo_3$ and 39.90° for $Pt_5Ru_3Mo_2$ catalysts, which are identical or slightly higher than that of pure Pt as shown in Fig. 3. These results show that Ru and Mo were not alloyed with Pt. The addition of Mo precursors

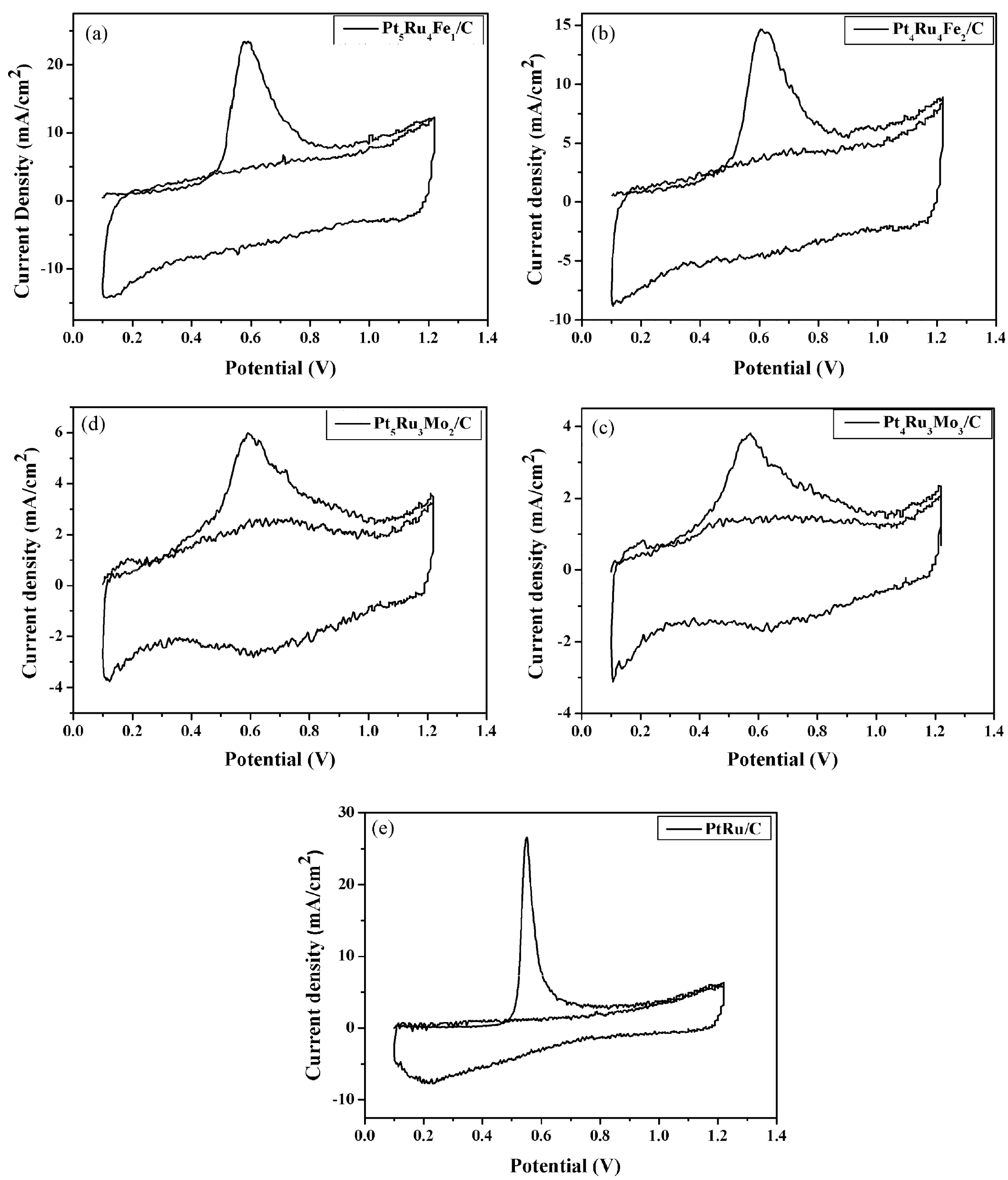

Fig. 4. CO stripping voltammetry of the catalysts: (a) $Pt_5Ru_4Fe_1/C$, (b) $Pt_4Ru_4Fe_2/C$, (c) $Pt_4Ru_3Mo_3/C$, (d) $Pt_5Ru_3Mo_2/C$, and (e) PtRu/C.

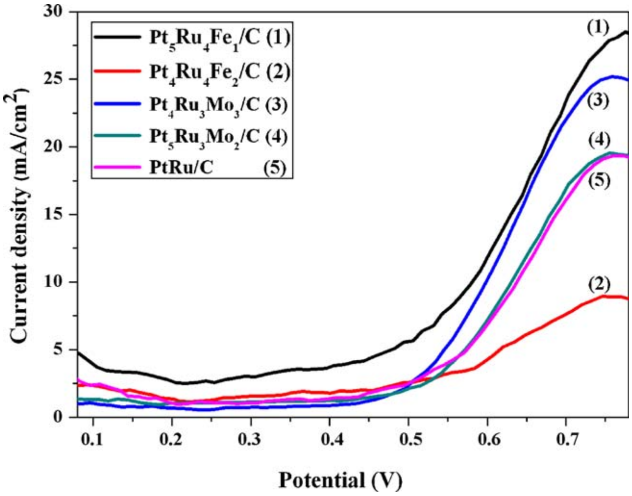

Fig. 5. MOR activity of the powder catalysts: $Pt_5Ru_4Fe_1/C$, $Pt_4Ru_4Fe_2/C$, $Pt_4Ru_3Mo_3/C$, $Pt_5Ru_3Mo_2/C$, and PtRu/C.

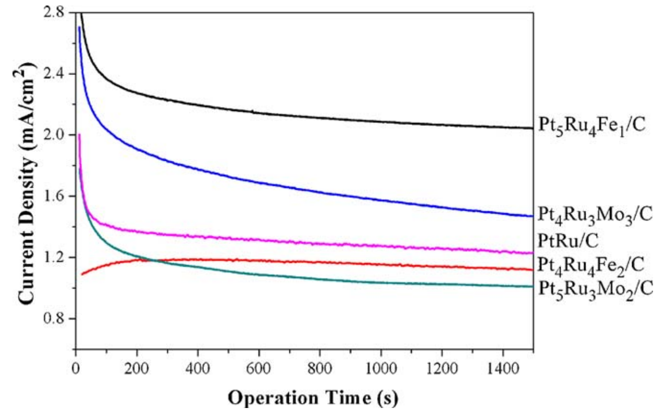

Fig. 6. Chronoampherometry measurements of the powder catalysts: $Pt_5Ru_4Fe_1/C$, $Pt_4Ru_4Fe_2/C$, $Pt_4Ru_3Mo_3/C$, $Pt_5Ru_3Mo_2/C$, and PtRu/C.

hindered alloying of Ru with Pt. As reported in a recent review on the preparation of ternary catalysts [14], generally the actual Pt:Ru atomic ratio in ternary PtRuM/C catalysts is close to that actual Pt:Ru atomic ratio of the binary PtRu/C catalyst, with the same nominal Pt:Ru composition, prepared by the same method, i.e. the actual Pt:Ru atomic ratio is not influenced by the presence of M atoms. The amount of Ru atoms alloyed with Pt atoms, instead, can be affected by the presence of a third metal [14]. This should explain the XRD results regarding the PtRuMo/C catalysts. Crystallite sizes, calculated by Scherrer equation [50], were 3.1, 3.0, 2.9, 3.3, and 3.4 nm for the PtRu/C, $Pt_5Ru_4Fe_1$, $Pt_4Ru_4Fe_2$, $Pt_4Ru_3Mo_3$, and $Pt_5Ru_3Mo_2$ catalysts, respectively. A summary of the XRD results is listed in Table 3.

The CO stripping results of the powder version catalysts are shown in Fig. 4. The on-set potential for CO electro-oxidation was analyzed to verify the effect of third metal on the CO electro-oxidation activity. In the PtRuFe catalysts, the on-set potential was observed at 0.40 V which is slightly lower than 0.45 V in the PtRu/C catalyst arising from the electro-withdrawing effect of Fe [12]. On the other hand, the PtRuMo catalysts exhibited significantly lower on-set potential at 0.30 V. The addition of Mo as a third metal improved CO electro-oxidation activity, resulting in the extensive suppression of CO poisoning during MOR. Electrochemically active surface area (EAS) was calculated by integrating the CO electro-oxidation peak of Fig. 4. The integrated area was converted to the EAS based on 420 $\mu C/m^2$ charge for monolayer CO. The calculated EAS value was 25.9 m^2/g-catal. for PtRu/C catalyst. The EAS values of $Pt_5Ru_4Fe_1$ and $Pt_4Ru_4Fe_2$ catalysts were 46.1 and 31.0 m^2/g-catal., respectively. It can be suggested that the higher activity of PtRuFe catalysts is arising from the increase in EAS. On the other hand, the PtRuMo catalysts exhibited noticeably reduced EAS values of 9.0 and 13.7 m^2/g-catal. for $Pt_5Ru_3Mo_2$ and $Pt_4Ru_3Mo_3$ catalysts, respectively. It can be concluded that enhanced catalytic activity of PtRuMo catalysts is due to the less poisoning of CO.

The MOR activities of the powder version catalysts are shown in Fig. 5. To evaluate the MOR activity, current densities of all catalysts were compared at 0.5 V. The current density of the PtRu/C catalyst was 1.50 mA/cm^2, while those of the ternary composition catalysts were 2.98, 1.31, 1.89, and 1.22 mA/cm^2 for the $Pt_5Ru_4Fe_1$, $Pt_4Ru_4Fe_2$, $Pt_5Ru_3Mo_2$, and $Pt_4Ru_3Mo_3$ catalysts, respectively. Mass and area-specific activities were calculated from the total metal loading and EAS values, and listed in Table 4. Among the ternary catalysts, the $Pt_5Ru_4Fe_1/C$ (2600 mA/g-catal.) and $Pt_4Ru_3Mo_3/C$ (1650 mA/g-catal.) catalysts showed higher mass activities than the commercial PtRu/C catalyst (1310 mA/g-catal.). Especially high mass activity (98% higher than that of the PtRu/C catalyst) was observed in the $Pt_5Ru_4Fe_1$ catalyst due to low on-set potential for CO electro-oxidation and much larger EAS. By adding Fe to PtRu, the EAS value increased from 25.9 m^2/g-catal. in the PtRu/C catalyst to 46.1 m^2/g-catal. in the $Pt_5Ru_4Fe_1$ catalyst, similar to the results of our previous study [12]. The $Pt_4Ru_3Mo_3$ catalyst showed higher mass activity by 26% than the PtRu/C catalyst. However, EAS of $Pt_4Ru_3Mo_3$ was less by 65% than that of PtRu/C. The area-specific activity of $Pt_4Ru_3Mo_3$ (184 mA/m^2) is higher by 260% than that of PtRu/C (50.8 mA/m^2). This result suggests that incorporation of Mo is beneficial for easy removal of CO. It should be noted that the on-set potentials of the ternary catalysts for the MOR were not lowered as much they did for the CO stripping experiments. This result suggests that the on-set potential for the MOR is not in direct match with that for the CO stripping reaction [51].

The MOR activities of the powder version catalysts with cyclicvoltammetry are compared with chronoampherometry results in Fig. 6 to eliminate the effect of capacitive current. $Pt_5Ru_4Fe_1$ catalyst has higher double layer capacitance than other catalysts. There is possibility that MOR current at 0.5 V of CV would be affected by double layer capacitance. After 1500 s testing at

Table 4
Summary of electrochemical property of the powder version catalysts.

Catalysts	EAS (m^2/g-catal.)	On-set potential for CO oxidation (V)	MOR activity measured by CV			MOR activity measured by chronoamperometry		
			Current density at 0.5 V (mA/cm^2)	Mass activity at 0.5 V (mA/g-catal.)	Area-specific activity at 0.5 V (mA/m^2)	Current density at 1500 s (mA/cm^2)	Mass activity at 1500 s (mA/g-catal.)	Area-specific activity at 1500 s (mA/m^2)
PtRu/C	25.9	0.45	1.50	1310	50.8	1.22	1060	40.9
$Pt_5Ru_4Fe_1/C$	46.1	0.40	2.98	2600	56.4	2.00	1750	38.0
$Pt_4Ru_4Fe_2/C$	31.0	0.40	1.31	1140	36.7	1.12	980	31.6
$Pt_4Ru_3Mo_3/C$	9.02	0.30	1.89	1650	182.9	1.53	1340	148
$Pt_5Ru_3Mo_2/C$	13.7	0.30	1.22	1070	78.1	1.01	884	64.4

0.5 V, current densities were 1.22, 2.00, 1.12, 1.53 and 1.01 mA/cm^2 for PtRu/C $Pt_5Ru_4Fe_1$, $Pt_4Ru_4Fe_2$, $Pt_5Ru_3Mo_2$, and $Pt_4Ru_3Mo_3$ catalysts, respectively. Mass activities after 1500 s testing were calculated from current densities and showed same trend with current densities. $Pt_5Ru_4Fe_1$ (1750 mA/g-catal.) and $Pt_4Ru_3Mo_3$ (1340 mA/g-catal.) show activities higher than PtRu/C (1060 mA/g-catal.). The high activity of the $Pt_5Ru_4Fe_1$ and $Pt_5Ru_3Mo_2$ catalysts was also observed in the chronoamperometry experiments. The order of the MOR activity was same as $Pt_5Ru_4Fe_1 > Pt_5Ru_3Mo_2 > PtRu/C > Pt_4Ru_4Fe_2 > Pt_4Ru_3Mo_3$ in both the cyclic and chronoamperometry tests, indicating that chronoamperometry tests are good in agreement with CV test.

From electrochemical characterization of powder version catalysts, $Pt_5Ru_4Fe_1$ and $Pt_4Ru_3Mo_3$ catalysts had higher MOR mass activity than the PtRu/C catalysts. The two other ternary catalysts, $Pt_4Ru_4Fe_2$ and $Pt_5Ru_3Mo_2$ in their powder version, showed mass activities lower than the PtRu/C catalyst, while $Pt_4Ru_4Fe_2$ and $Pt_5Ru_3Mo_2$ prepared for combinatorial library showed mass activities higher than PtRu/C. This difference must be due to the different synthesis condition between the combinatorial library and the powder version catalysts, such as mixing and the sequence of metal precursor impregnation. Because of small volume of each spots in the combinatorial library, metal precursors in solutions cannot be agitated and metal precursor solutions have to be added sequentially. However, high degree of mixing and simultaneous addition of each metal precursor was accomplished during the preparation of powder version catalyst.

4. Conclusions

Composition optimization of the ternary PtRuFe and PtRuMo systems was performed via combinatorial synthesis and high-throughput screening method. A more reliable version of combinatorial library was synthesized by dripping catalyst precursors on carbon powders to make the library spots in a close manner to the powder form catalyst synthesis method. In the combinatorial library, $Pt_5Ru_4Fe_1$, $Pt_4Ru_4Fe_2$, $Pt_5Ru_3Mo_2$, and $Pt_4Ru_3Mo_3$ compositions exhibited high MOR activities. The highest mass activity was observed in $Pt_5Ru_4Fe_1$/C catalyst, which was 98% higher than that of the PtRu/C. The area-specific activity of the $Pt_4Ru_3Mo_3$/C catalyst was higher by 260% than the PtRu/C catalyst.

Acknowledgements

The authors are thankful to Dr. W.C. Choi in Korea Research Institute of Chemical Technology for his support and guidance. This work was funded by the Center for Ultramicrochemical Process Systems (CUPS) sponsored by KOSEF (2009). This work was supported by the Korea Science & Engineering Foundation (KOSEF) grant (WCU program, 31-2008-000-10055-0) funded by the Ministry of Education and Science & Technology (MEST).

References

[1] M. Baldauf, W. Preidel, J. Power Sources 84 (1999) 161–166.
[2] H. Liu, C. Songa, L. Zhang, J. Zhang, H. Wang, D.P. Wilkinson, J. Power Sources 155 (2006) 95–110.
[3] O.A. Petrii, J. Solid-State Electrochem. 12 (2008) 609–642.
[4] W.C. Choi, M.K. Jeon, Y.J. Kim, S.I. Woo, W.H. Hong, Catal. Today 93–95 (2004) 517–522.
[5] W.C. Choi, S.I. Woo, M.K. Jeon, J.M. Sohn, M.R. Kim, H.J. Jeon, Adv. Mater. 17 (2005) 446–451.
[6] A.S. Arico, S. Srinivasn, V. Antonucci, Fuel Cells 1 (2001) 133–161.
[7] W.C. Choi, J.D. Kim, S.I. Woo, J. Power Sources 96 (2001) 411–414.
[8] N.M. Markovic, H.A. Gasteiger, P.N. Ross Jr., Electrochim. Acta 40 (1995) 91–98.
[9] M. Watanabe, S. Motoo, J. Electroanal. Chem. 60 (1975) 267–273.
[10] J. Luo, L. Wang, D. Mott, P.N. Njoki, Y. Lin, T. He, Z. Xu, B.N. Wanjana, I.S. Lim, C.J. Zhong, Adv. Mater. 20 (2008) 4342–4347.
[11] N. Kristian, X. Wang, Electrochem. Commun. 10 (2008) 12–15.
[12] M.K. Jeon, J.Y. Won, K.R. Lee, S.I. Woo, Electrochem. Commun. 9 (2007) 2163–2166.
[13] J.H. Choi, K.W. Park, B.K. Kwon, Y.E. Sung, J. Electrochem. Soc. 150 (2003) A973–A978.
[14] E. Antolini, Appl. Catal. B: Environ. 74 (2007) 337–350.
[15] S. Pasupath, V. Tricoli, J. Solid-State Electrochem. 12 (2008) 1093–1100.
[16] W.C. Choi, J.D. Kim, S.I. Woo, Catal. Today 74 (2002) 235–240.
[17] W.C. Choi, S.I. Woo, J. Power Sources 124 (2003) 420–425.
[18] C. Kim, H.H. Kwon, I.K. Song, Y.E. Sung, W.S. Chung, H.I. Lee, J. Power Sources 171 (2007) 404–411.
[19] G. Yu, W. Chen, J. Zhao, Q. Nie, J. Appl. Electrochem. 36 (2006) 1021–1025.
[20] U.B. Demirci, J. Power Sources 173 (2007) 11–18.
[21] M.K. Jeon, J.S. Cooper, P.J. McGinn, J. Power Sources 185 (2008) 913–916.
[22] Z.B. Wang, G.P. Yin, P.E. Shi, Y.C. Sun, Electrochem. Solid-State Lett. 9 (2006) A13–A15.
[23] K.I.B. Eguiluz, G.R. Salazar-Banda, D. Miwa, S.A.S. Machado, L.A. Avaca, J. Power Sources 179 (2008) 42–49.
[24] J.S. Cooper, P.J. McGinn, J. Power Sources 163 (2006) 330–338.
[25] M. Goetz, H. Wendt, J. Appl. Electrochem. 31 (2001) 811–817.
[26] P. Strasser, J. Comb. Chem. 10 (2008) 216–224.
[27] M.K. Jeon, K.R. Lee, H. Daimon, A. Nakahara, S.I. Woo, Catal. Today 132 (2008) 123–126.
[28] M.K. Jeon, K.R. Lee, S.I. Woo, J. Korean, Chem. Eng. 26 (2009) 1028–1033.
[29] T.Y. Morante-Catacora, Y. Ishikawa, C.R. Cabrera, J. Electroanal. Chem. 621 (2008) 103–112.
[30] A. Bauer, E.L. Gyenge, C.W. Oloman, J. Power Sources 167 (2007) 281–287.
[31] M. Watanabe, H. Igarashi, T. Fujino, Electrochemistry 67 (1999) 1194–1196.
[32] N.P. Lebedeva, G.J.M. Janssen, Electrochim. Acta 51 (2005) 29–40.
[33] E.I. Santiago, G.A. Camara, E.A. Ticianelli, Electrochim. Acta 48 (2003) 3527–3534.
[34] E. Reddington, A. Sapienza, B. Gurau, R. Viswanathan, S. Sarangapani, E.S. Smotkin, T.E. Mallouk, Science 280 (1998) 1735–1737.
[35] J.F. Whitracre, T. Valdez, S.R. Narayanan, J. Electrochem. Soc. 152 (2005) A1780–A1789.
[36] S. Jayaraman, S.H. Baeck, T.F. Jaramillo, A. Kleinman-Shwarsctein, E.W. McFarland, Rev. Sci. Instrum. 76 (2005) 062227.
[37] J.H. Liu, M.K. Jeon, S.I. Woo, Appl. Surf. Sci. 252 (2006) 2580–2587.
[38] M. Black, J. Cooper, P. McGinn, Meas. Sci. Technol. 16 (2005) 174–182.
[39] S. Guerin, B.E. Hayden, C.E. Lee, C. Mormiche, J.R. Owen, A.E. Russel, J. Comb. Chem. 6 (2004) 149–158.
[40] M.D. Fleischauer, T.D. Hatchard, G.P. Rockwell, J.M. Topple, S. Trussler, S.K. Jericho, M.H. Jericho, J.R. Dahn, J. Electrochem. Soc. 150 (2003) A1465–A1469.
[41] R. Liu, E.S. Smotkin, J. Electroanal. Chem. 535 (2002) 49–55.
[42] E.S. Smotkin, J. Jiang, A. Nayar, R. Liu, Appl. Surf. Sci. 252 (2006) 2573–2579.
[43] M.K. Jeon, K.R. Lee, W.S. Lee, H. Daimon, A. Nakahara, S.I. Woo, J. Power Sources 185 (2008) 927–931.
[44] R. Jiang, D. Chu, J. Electroanal. Chem. 527 (2002) 137–142.
[45] T.J. Schmidt, H.A. Gasteiger, G.D. Stäb, P.M. Urban, D.M. Kolb, R.J. Behm, J. Electrochem. Soc. 145 (1998) 2354–2358.
[46] H.A. Gasteiger, N. Markovic, P.N. Ross Jr., E.J. Cairns, J. Electrochem. Soc. 141 (1994) 1795–1803.
[47] J.B. Goodenough, R. Manoharan, A.K. Shukla, K.V. Ramesh, Chem. Mater. 1 (1989) 391–398.
[48] A.J. Dickinson, L.P.L. Carrette, J.A. Collins, K.A. Friedrich, U. Stimming, J. Appl. Electrochem. 34 (2004) 975–980.
[49] J. Xu, K. Hua, G. Sun, C. Wang, X. Lu, Y. Wang, Electrochem. Commun. 8 (2006) 982–986.
[50] C.Z. He, H.R. Kunz, J.M. Fenton, J. Electrochem. Soc. 144 (1997) 970–979.
[51] D.R.M. Godoi, J. Perez, H. Mercedes Villuas, J. Phys. Chem. C 113 (2009) 8518–8525.